

Satellites promise global-scale quantum networks

SUMIT GOSWAMI,^{1,2,*} SAYANDIP DHARA,³ NEIL SINCLAIR,^{4,5} MAKAN MOHAGEG,⁶
JASMINDER S. SIDHU,⁷ SABYASACHI MUKHOPADHYAY,⁸ MARKUS KRUTZIK,^{9,10}
JOHN R. LOWELL,⁶ DANIEL K. L. OI,⁷ MUSTAFA GÜNDOĞAN,⁹ YING-CHENG CHEN,¹
HSIANG-HUA JEN,^{1,11} AND CHRISTOPH SIMON^{2,12}

¹*Institute of Atomic and Molecular Sciences, Academia Sinica, Taipei City, Taiwan*

²*Institute for Quantum Science and Technology, and Department of Physics & Astronomy, University of Calgary, 2500 University Drive NW, Calgary, Alberta T2N 1N4, Canada*

³*Virginia Tech, Blacksburg, Virginia 24061, USA*

⁴*John A. Paulson School of Engineering and Applied Science, Harvard University, 29 Oxford St, Cambridge, Massachusetts 02138, USA*

⁵*Division of Physics, Mathematics and Astronomy, and Alliance for Quantum Technologies (AQT), California Institute of Technology, 1200 E. California Blvd., Pasadena, California 91125, USA*

⁶*Boeing Research and Technology, 929 Long Bridge Drive, Arlington, Virginia 22202, USA*

⁷*SUPA Department of Physics, University of Strathclyde, Glasgow G4 0NG, UK*

⁸*Centre for Computational and Data Sciences, IIT Kharagpur, Kharagpur, West Bengal 721302, India*

⁹*Institut für Physik and Center for the Science of Materials Berlin (CSMB), Humboldt-Universität zu Berlin, Newtonstr. 15, Berlin 12489, Germany*

¹⁰*Ferdinand-Braun-Institut (FBH), Gustav-Kirchoff-Str. 4, Berlin 12489, Germany*

¹¹*Physics Division, National Center for Theoretical Sciences, Taipei City, Taiwan*

¹²*csimo@ucalgary.ca*

*sumitgoswami@gate.sinica.edu.tw

Received 13 May 2025; revised 4 September 2025; accepted 4 November 2025; published 16 December 2025

Academia, governments, and industry around the world are on a quest to build long-distance quantum communication networks for a future quantum internet. Using air and fiber channels, quantum communication quickly faced the daunting challenge of exponential photon loss with distance. Quantum repeaters were invented to solve the loss problem by probabilistically establishing entanglement over short distances and using quantum memories to synchronize the teleportation of such entanglement to long distances. However, due to imperfections and complexities of quantum memories, ground-based proof-of-concept repeater demonstrations have yet been restricted to metropolitan-scale distances. In contrast, direct photon transmission from satellites through empty space faces almost no exponential absorption loss and only quadratic beam divergence loss. A single satellite successfully distributed entanglement over more than 1,200 km. It is becoming increasingly clear that quantum communication over large intercontinental distances (e.g., 4,000–20,000 km) will likely employ a satellite-based architecture. This could involve quantum memories and repeater protocols in satellites, or memory-less satellite-chains through which photons are simply reflected, or some combination thereof. Rapid advancements in the space launch and classical satellite communications industry provide a strong tailwind for satellite quantum communication, promising economical and easier deployment of quantum communication satellites.

© 2025 Optica Publishing Group under the terms of the [Optica Open Access Publishing Agreement](#)

<https://doi.org/10.1364/OPTICAQ.567531>

1. INTRODUCTION

Quantum communication networks are emerging as an advanced communication technology while also offering new avenues for fundamental physics research [1]. A quantum network enabling the transfer of quantum information anywhere on Earth, i.e., a quantum internet, would transform many current and future technologies. Among these technologies are quantum cryptography, quantum sensing and timekeeping, as well as distributed quantum computing [2–11]. A form of quantum cryptography, quantum key distribution (QKD), provides information-

theoretic security based on the laws of quantum physics [2–4]. QKD relies on the distribution and measurement of both separable and entangled qubits and is the most near-term application of quantum communication in which significant progress has already been made [5]. Distributed entanglement for quantum sensing includes improved precision of long baseline telescopes [8] and entangled atomic clocks for improved timekeeping or navigation [9]. In distributed quantum computing, multiple otherwise independent quantum computers are connected to achieve computation in a much larger Hilbert space and allow

multi-party computational protocols [6,10–12]. Other cryptographic primitives in quantum networks include blind quantum computing [13–15], private database queries [16,17], and quantum secret sharing [18]. Blind quantum computing allows users to run quantum computations on a remote server without revealing their inputs, computation, or results. Private database queries enable the retrieval of specific information from a database without disclosing the query itself to the database owner. Quantum secret sharing distributes a secret quantum state among multiple parties, requiring collaboration to reconstruct it, ensuring security and resilience to the loss of a subset of parties. Fundamental physics research with quantum networks include tests of quantum mechanics like Bell inequality violations at large distances [19,20] and simultaneous tests of quantum mechanics and general relativity [21–25].

Information in quantum networks is carried by photonic quantum states. The principal issue hindering the development of a quantum network is photon loss and, depending on the application, information errors. Since quantum mechanics forbids qubit cloning (i.e., copying) to overcome loss [26–28], several other methods have been investigated. One way is to merely generate qubits at a high rate and directly transmit them through fiber or air [29]. However, this approach is practically constrained to short distances due to attenuation through these channels. Optical attenuation loss in fiber or air scales exponentially with distance. For example, optical fibers designed for low-loss classical communications have an attenuation coefficient as low as 0.16 dB/km (Corning Vascade). This corresponds to a loss of 100 dB or 10^{-10} in 625 km (distance from Boston to Washington D.C.), corresponding to only 1 Hz transmission rate for a 10 GHz source [30]. The effect of attenuation and atmospheric turbulence, not to mention the curvature of the Earth, has limited the distance of experiments in ground-to-ground free-space optical links through air to only around 150 km [5,31].

Quantum repeaters were proposed [32] to distribute entanglement over long and/or lossy channels by utilizing quantum memories. Once entanglement is distributed, it is used directly or for teleporting quantum information. In most repeater protocols, photons travel short distances to generate entanglement between near-separated quantum memories. Entanglement between these memories is converted into entanglement between widely separated memories through entanglement swapping [1,33,34]. In this way, an improved loss scaling can be achieved over fiber and air, in principle. However, other than entanglement sources, repeaters also require high-performance quantum memories which, despite years of impressive progress, are still a significant technological bottleneck for practical implementations. There have been only a few repeater (sub-link) demonstrations that surpass the performance of direct transmission [35,36]. But rates are impractical and deployment in the field has been limited, although progress has been made in these directions [37–39]. Moreover, the simplest repeater protocols (sometimes referred to as “first-generation” repeaters [40]) cannot reliably distribute quantum information beyond a certain distance (e.g., 2,000 km) due to the accumulation of errors and increasing experimental complexities of the repeater protocol [1]. Other repeater concepts under development [41], called second- and third-generation repeaters [40,42] use quantum error correction to further extend distances [43], including all-photonic repeaters

[44–46] that aim to eliminate quantum memories entirely in a repeater. However, these protocols require extensive resources and frequent repeater stations [47,48].

Optical attenuation inside a medium (e.g., air or fiber) is not necessarily a limiting factor for global-scale quantum communication, if a communication medium with low attenuation loss is used. However, it is challenging to create new kinds of optical fibers. For instance, if long experimental fluoride glass fibers with theoretically predicted minimum loss of $6.5 * 10^{-3}$ dB/km [49] could be created and produced in a scalable way, global-scale (i.e., 20,000 km) transmission would still have about 130 dB loss. Although such fibers can have low loss (in tens of dB) when used for quantum networks over thousands of kilometers, currently, they still have higher losses than silica fibers. An alternative to direct transmission is sending light through a vacuum. This can be the vacuum of outer space accessed through satellite transmissions, which form the core subject of this review. Another recently proposed direction is “vacuum beam guide” channels through evacuated tubes, potentially buried into the earth [50], although they would potentially face enormous construction, political, and financial challenges.

Transmission of quantum information using satellites has been remarkably successful, and research is progressing rapidly [19,51–54]. Photonic qubits mostly travel through empty space without any exponential attenuation loss, due to lack of a medium. The only attenuation loss associated with satellite transmission is the short distance (~ 20 km) light needs to travel into and out of the earth’s atmosphere for connecting ground stations. For vertical transmission (i.e., at zenith) at 1550 nm telecommunication wavelength, atmospheric attenuation loss is around 10% (or 0.5 dB) [55]. Photons from satellites instead face diffraction loss or beam divergence loss, which increases only quadratically with distance. Due to this major advantage, the Micius satellite launched by China in 2016 achieved a groundbreaking entanglement distribution distance of 1,200 km [19] and performed entanglement-based QKD over 1,120 km [51], going much further beyond optical fibers. However, due to Earth’s curvature, single satellites in low-earth orbit (LEO, 200–2000 km altitude) like Micius have a visibility of the Earth only up to a maximum of a few thousand km. In addition, highly oblique (i.e., near-tangential) transmission through the atmosphere experiences higher absorption losses, further limiting range. To reach longer distances one may employ satellites in higher orbits like geostationary orbits (at 36,000 km). However, such high orbits will cause large diffraction loss and consequently achieve low rates. This method is also associated with high communication latency time with the satellite. To reach intercontinental and global distances (say, 4,000 to 20,000 km), several quantum repeater proposals combining satellites and quantum memories have been put forward. This includes architectures with quantum memories in ground stations [56] or on-board satellites [57,58], including schemes where satellites move to transfer stored photons [1,59]. Recently, a simpler architecture was proposed to achieve global-scale entanglement distribution by just reflection, without requiring quantum memories or repeaters [60]. This optical relay approach utilizes a synchronously moving satellite chain where light is refocused at each satellite in the chain and transmitted to the next. Such a relay confines beam divergence indefinitely akin to a set of lenses

on an optical bench. Such proposals, combined with rapidly advancing satellite experiments, diversify the possible mission architectures for deploying satellite-based quantum networks.

Satellite-based quantum communications are poised to leverage the rapid progress in the space industry, including low launch costs offered by reusable rocket technology [61–66] and an exponentially growing constellation of satellites [67–70]. This offers lower cost and easier launches for quantum satellite networks and broader implementations of quantum technologies in space.

In this review, we first overview quantum repeaters and their challenges. This motivates satellite-based quantum communication. We then introduce satellites and discuss their advantages and limitations. Low-earth orbit satellite experiments using *Micrus* are discussed. To achieve longer distances, several protocols are discussed, including those that use satellites and quantum memories. Finally, the satellite relay is introduced, discussing its benefits and challenges, including comparison to the ground-based relay proposal called vacuum beam guides. Before concluding, we explore the potential of a combined relay-repeater network. Parts of this review are inspired by the quantum network discussions in Ref. [71].

2. QUANTUM REPEATERS

The goal of a quantum network is to distribute quantum information between different locations that can be separated by long and/or lossy channels. Quantum repeaters are designed to solve the photon loss problem by cleverly synchronizing the distribution and teleportation of entanglement over a channel using quantum memories. Then, quantum information can be transferred by teleportation using the entanglement established between the endpoints of the channel. The concept of a quantum repeater is shown in Fig. 1. The basic scheme of teleportation, upon which quantum repeaters rely on, is shown in Fig. 1(a). The state of one qubit (1) is teleported to a distant qubit (3) entangled with another qubit (2) when a joint measurement is performed on qubits 1 and 2. This requires pre-established entanglement between distant qubits 2 and 3. The joint measurement consists of an entangling gate followed by measurement (shown by a green dashed ellipse), which can be implemented using linear optics or matter qubits. Afterwards, the measurement result is classically transmitted to properly interpret qubit 3 and complete the teleportation.

In a quantum repeater, entanglement is distributed over several short segments of the channel, and a chain of successive teleportation events between one of the qubits from each entangled state leads to entanglement being established between the ends of the channel. This is shown in Fig. 1(b) for dividing the channel into two segments; the state of II is teleported to IV. Such teleportation of entanglement is also referred to as entanglement swapping. However, one can only perform teleportation if the joint measurement (between II and III in Fig. 1(b)) succeeds, that is, the entangled qubits must not be lost during their distribution over the short segments. The probability of this occurring directly (without storage in memories) is equivalent to a single photon successfully traversing the entire channel (from I to IV in Fig. 1(b)), rendering the teleportation approach no more effective than direct transmission.

Quantum memories address this challenge by storing entangled qubits until entanglement is successfully generated

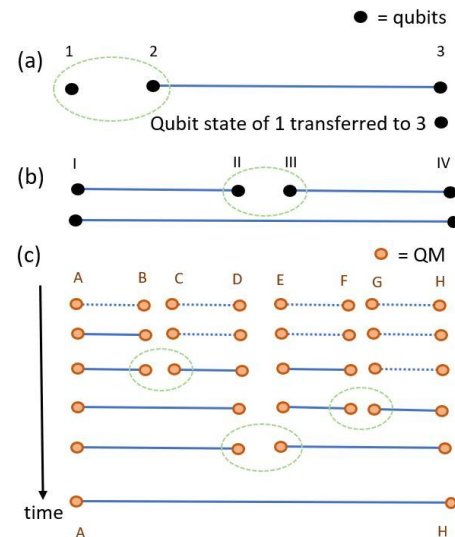


Fig. 1. (a) Teleportation—Initially distant qubits 2 and 3 are entangled (shown by solid blue line), while qubit 1 is separate with its own quantum state but physically close qubit 2. In the next step, the qubit state of 1 is teleported to the distant qubit 3 by doing a joint operation on qubits 1 and 2. This operation (shown by green dashed circle) consists of an entangling gate followed by measurement. For photonics qubits this can be Bell-state measurement, while for atomic qubits it is a two-qubit entangling gate followed by measurement. Further classical communication of the measurement results and single qubits gates on qubit 3 based on the measurement results is needed to complete the teleportation process. This is not shown in the figure for simplicity and mentioned in detail in text. (b) Teleporting an entangled qubit (say II here) to a distant location (say, at the place of IV) forms the basis of a quantum repeater. This enables entangled distribution over longer distances. (c) A schematic diagram showing the working principle of quantum repeaters. Initially, eight quantum memories (A–H) are not connected to each other. Eventually, entanglement between A and H was established through successive tries of entanglement generation, storing and eventually performing the entanglement swapping operation (See text for details). The figure is reproduced from [71] with permission.

across neighboring segments in a quantum repeater. This synchronizes the arrival of the entangled qubits for the required joint measurements for teleportation/swapping, and heralding thereof, which extends the entanglement over longer distances. Figure 1(c) illustrates this process. Initially, eight separated quantum memories (A–H) attempt to establish entanglement between neighboring pairs (e.g., A–B, C–D). Successful attempts are stored while failed ones (e.g., C–D in the first attempt) are repeated. Once adjacent pairs are entangled (e.g., A–B and C–D), joint entangling measurements are performed on nearest neighbor qubits (e.g., B and C) resulting in entanglement being established over longer distances (e.g., A and D). This process continues, ultimately entangling the endpoints (A and H). Although simplified, this example demonstrates the fundamental principle of quantum repeaters.

In our example, the longest time certain quantum memories (e.g., memory A) need to store a qubit is from the time entanglement is first created in the memory until entanglement distribution in the whole link is finished. Hence, quantum memories must have long storage times. Depending on the architecture, the minimum storage time ranges from seconds to a millisecond,

and is fundamentally bounded by the light travel time in the short segments. The length of each segment must also be long enough for practical use and to avoid the compounding effects of imperfections at the storage and swapping steps. Quantum memories must also be efficient and low noise, accommodate a reasonable entanglement distribution rate, ideally store a large number of entangled modes, and must be compatible with the entangling operation step. These properties are crucial, as only a few entangled pairs are successfully stored out of the many photons sent, even when near-ideal quantum memories are used [1,33]. The entanglement generation rate can also be linearly increased using multiplexing of memories and channels, e.g., through the use of additional spatial, temporal, or spectral modes. The strict requirements on the quantum memories represent one of the most significant barriers towards successful implementation of a quantum repeater. Milestone properties have been individually approached in separate quantum memories [72], but not all together in a single device. For instance, ultracold atomic memories and solid-state memories have both achieved over 100 ms storage time [73–75] and separately above 90% efficiency in ultracold atoms [76,77]. On the other hand, rare-earth ion doped atomic frequency comb quantum memories have achieved large multiplexing capacity by storing as many as 1650 separate single photon modes [78–80]. Silicon vacancy centers in diamond have demonstrated a repeater that improves over direct transmission, but these memories are low rate and currently lack multiplexing capabilities [35]. In later sections in this review, we will discuss quantum memories in the context of those that store and retrieve externally provided photons, although different types of memories, e.g., those that produce probabilistic or deterministic spin-photon entanglement, may be used in principle with suitable protocol modification.

The fundamental structure of the quantum repeater described above was proposed by Briegel *et al.* [32]. One of the early proposals to implement such a quantum repeater using atomic ensembles and heralded entanglement generation was proposed in 2001 by Duan *et al.* [34], widely known as the DLCZ protocol. Although seminal, the limitations of DLCZ include low rates to avoid creation of multiphoton-pair events, inefficient heralding, lack of multiplexing, and operation at visible wavelengths, which is incompatible with long-distance fiber transmission, in addition to the challenge of achieving high-performance quantum memory [81,82]. To solve these and other problems, many different repeater schemes have been designed over the years [83–87]. For example, one of these uses a non-degenerate entangled photon pair source [88] and multiplexed memories. One of the photons emitted by the entanglement source is at telecom wavelengths to be sent to long distances, whereas its pair photon can be at a suitable wavelength for storage in quantum memory [89,90]. The quantum memories and entanglement sources used in many quantum repeater proposals are based on (bulk) ensemble systems, such as cold atoms and nonlinear crystals, respectively. Repeaters using individual quantum systems (i.e., single atoms, ions, color centers in diamond, quantum dots, etc.) for entanglement generation and storage have also experienced a lot of attention and progress [20,35,38,91–96]. The principal scheme is generally similar: creating and or storing excitations in remote stations, and upon readout, projecting them into an entangled state by erasing the which-way information that the photons possess [20]. The primary advantage of single systems over ensembles is suppression of multi-photon events

and noise, deterministic gates, and built-in qubits for error correction [34,35,97]. However, such systems can be hard to create at scale, and hence have been challenging to interface and multiplex, in addition to requiring carefully constructed cavities to enhance light-matter coupling.

Research on quantum repeaters and physical systems to construct them is ongoing. In the meantime, proof-of-concept quantum repeater has been implemented in lab settings and also recently in real-world scenarios over up to 50 km in several metropolitan areas [12,35,37–39,98–102]. However, quantum repeaters are just beginning to surpass the rate-loss bound [103] for direct transmission experiments that are outside of the lab [35,36,38]. A rate-loss bound is often used to distinguish direct transmission from a repeater independent of its specific components or protocol. Current demonstrations surpassing this bound have been very low-rate in that the demonstrations allowed non-zero transmission of qubits over a channel of exceptionally high loss, e.g., [35]. The bound is generally defined with respect to a single (non-multiplexed) channel or mode and does not take into account requirements to implement any specific protocol, e.g., QKD or distributed quantum computing.

Due to the complexities in their design and implementations, existing proof-of-concept repeater demonstrations generally fall into the first-generation quantum repeater category. There are other proposals [43] that employ quantum error correction in quantum repeaters to actively combat noise, called second-generation repeaters [40,42]. Error correction enables the distribution of higher-quality entanglement and allows reaching longer distances, in principle. There also exist proposals to eliminate the need for quantum memories altogether, called all-photonic repeaters [44], by sending a large encoded quantum states like graph states, which will be error-corrected for both channel loss and operation losses [45,46]. However, both of these alternatives have extremely high resource requirements and are only very early on in their development. For example, they require many qubits as resources and very frequent repeater stations, e.g., every 1–2 km [47]. Resource estimation shows that one needs 10^6 single photon sources per node, even when repeater stations are separated by just 1.5 km [48]. Due to the aforementioned challenges with repeater architectures, direct transmission of qubits from orbiting satellites has been investigated to reach large distances with high rates.

3. SATELLITES

Quantum communication satellite missions have achieved entanglement distribution over 1200 km [19] between two locations on earth, which is impossible currently with any fibre-based architecture. This has been possible as loss in satellite transmission is principally due to diffraction, which varies quadratically with distance as compared to the exponential attenuation loss in optical fibers or air transmission. Diffraction loss occurs due to beam divergence. This increases with communication distance and also depends on the transmitting and receiving telescope diameters. Large ground telescopes (meter diameters) are commonly used in space-to-ground quantum communication demonstrations. However, satellite telescopes are restricted to smaller sizes (in tens of cm) as large telescopes are expensive to deploy in orbit. Beam pointing error is also an important contributor to channel loss [104]. A LEO satellite circles the earth almost every 90 minutes at 8 km/s speed. Hence,

employing sophisticated satellite tracking technology is one of the most important parts of a satellite-based quantum communication mission [105].

Atmospheric transmission loss, due to absorption, scattering, and turbulence, is another significant factor. Absorption loss depends on the wavelength of light and the angle of incidence through the atmosphere [105]. Light to and from satellites that is incident at a very low elevation angle incurs dramatically increased attenuation as it traverses a long path through the atmosphere [106]. Turbulence generates random fluctuations in the refractive index of the air which results in beam spreading, beam wandering, and even beam fragmentation, causing loss. Turbulence is most pronounced close to the surface of the earth as the atmosphere is thickest closest to the Earth. After 20 km, the atmosphere itself is too thin to be considered. Generally, turbulence impacts uplink transmission to a greater extent than downlink transmission, because in uplink, the turbulence-induced beam, after emanating from the atmosphere, has to travel for hundreds of km to reach the satellite.

Adaptive optics systems can help compensate for turbulence by first surveying the atmosphere using a downlink reference light from the satellite and then introducing beam tilt and wavefront corrections to the outgoing uplink beam using segmented-mirror ground telescopes. Atmospheric turbulence effects occur on time scales of the order of 10–100 ms (but can be much shorter in some conditions). Laser pulses, and qubit wavepacket durations, are generally much shorter than that timescale, enabling them to properly survey and compensate for the refractive index variations. Such compensation does not work very well for uplinks as the downlink reference beam from satellite and the uplink beam containing the qubit cannot be in the same spatial mode due to the 8 km/s satellite motion. Better results can be obtained using laser guide stars (LGS) which are artificial stars created by exciting sodium in the mesosphere at around 90 km elevation using a powerful laser that follows satellite movement [107]. The light from this artificial moving star travels through the turbulent atmosphere to be detected on earth for compensation. These different adaptive optics methods, developed in classical optics (especially for astrophysical observations), provide partial solutions to the high channel loss issue in the uplink due to turbulence. In quantum communication, these techniques are inherited while making sure the quantum channels are not corrupted (i.e., qubit decoherence) due to the turbulence effect. Polarization [52] and time-bin [108] qubits can be used for quantum communication through the uplink channel.

LEO satellites—either in uplink or downlink—face the challenge of limited flyby times. These satellites typically move at speeds of around 8 km/s. For a satellite in a 500 km-distance orbit, assuming tracking over a 1,000 km distance, the flyby time is approximately 2 minutes. Tracking at higher elevation angles, where atmospheric loss is greater, can slightly extend this time, but it remains limited still to a few minutes for LEO satellites. While LEO satellites have shorter flyby times per ground station, their movement allows them to rapidly service different locations as they traverse their orbit. As the Earth also rotates below the rotating LEO satellite, a properly positioned LEO satellite can fly over every point on Earth within a specific interval. For example, a satellite in polar orbit will pass over and be able to transmit to any specific point on Earth at least twice each day, in clear weather. Quantum communication with LEO satellites can take advantage of this for addressing several sites across the world at regular fixed intervals.

The signal-to-noise ratio (SNR) plays a critical role in quantum communication. Noise shortens communication distances and restricts or prohibits quantum network functionalities. During daytime, reflected sunlight becomes the dominant noise source. Consequently, daytime operation of satellite QKD remains a challenge, as demonstrated by the Micius satellite, in which links are predominantly established at night. At night, the dominant noise source shifts to light pollution from cities. Therefore, ground stations located far from urban centers, where light pollution is minimized, are preferable for achieving optimal SNR. High SNR can be achieved by reducing background noise and/or increasing the signal strength, through reduced transmission loss, improved filtering, or enabling large multiplexing capacity for the signal [109,110]. For example, in a recent paper [111], a novel idea was proposed to enable daytime operations. The large background noise from sunlight can be reduced if the quantum signal employs particular wavelengths that are absent in the solar spectrum or have a very reduced intensity (e.g., the dark absorption lines or Fraunhofer lines) [111]. Adaptive optics systems have been used to reduce daytime noise in free-space-optical QKD channels too [112].

4. SATELLITE TRANSMISSION EXPERIMENTS

Prior to the Micius satellite launch, there were several feasibility studies to ascertain parameters like total loss or background noise in downlink or uplink transmission [105,113]. Initial experiments were also conducted using optical sources or retro-reflectors present in existing satellites [114–119]. These experiments investigated different parameters, including conclusively proving that a polarization qubit would not decohere due to turbulence in atmospheric transmission. In addition to these test experiments, retroreflectors can also achieve downlink qubit transmission by working as polarization converters to uplink weak laser pulses sent from ground to the satellite [119].

In 2017, in culmination of all the previous work, the Micius satellite was launched by China, which achieved several milestones: entanglement distribution over 1200 km [19], quantum teleportation to the satellite over 1400 km [52], and several successful QKD demonstrations [51,53,54,120,121]. The different experiments performed by Micius satellite are depicted in Fig. 2. Micius was equipped with two telescopes (with diameters 30 cm and 18 cm), PPKTP (Periodically Poled Potassium Titanyl Phosphate)-based SPDC (Spontaneous Parametric Down-Conversion) entangled photon source, a weak coherent pulse (WCP) source to carry out QKD schemes and single photon detectors. It also had more lasers, alignment optics, and detectors to be used for satellite tracking (acquiring pointing and tracking (APT) system) and polarization correction. Micius performed QKD in the downlink scenario using a WCP source through the BB84 protocol [53] and another downlink QKD protocol using an onboard entanglement source [120], as shown in Figs. 2(a) and 2(b). Micius also performed an uplink transmission experiment. As depicted in Fig. 2(c), one qubit from an entangled pair was uplinked to Micius, and an entangled photonic qubit was teleported/swapped from ground to the satellite over distances ranging between 500 and 1400 km [52]. Both entangled photon pairs were generated from the same pump laser for phase control and to ensure complete mode overlap of the photons on a beam splitter to implement the entangling

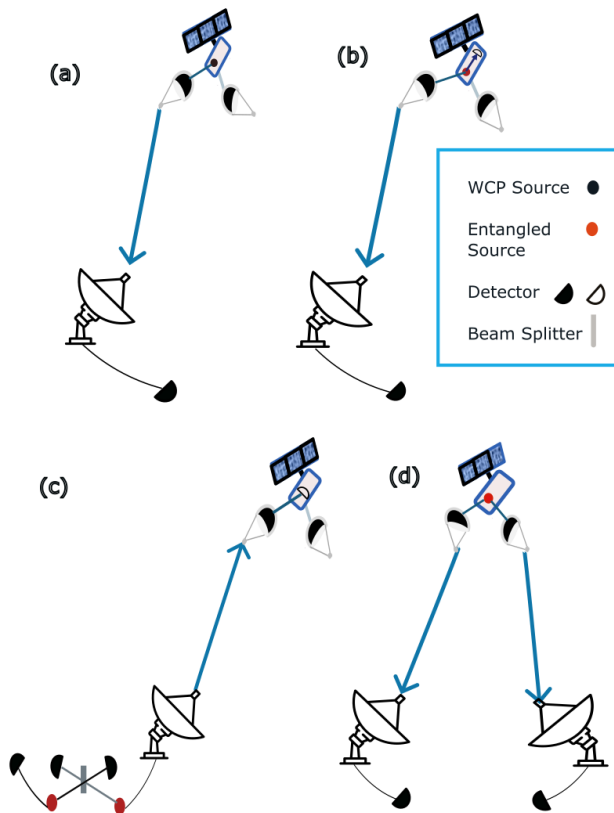


Fig. 2. Different experiments performed with the Micius satellite [19,52,53,120], as described in [71]. (a) Downlink QKD—Using a weak coherent pulse (WCP) source (black circle) photons are sent downlink to ground station to perform decoy-state QKD [53]. (b) Entanglement based QKD—An entangled pair source (red circle) aboard Micius is used to perform QKD between the satellite and the ground station. (c) Uplink teleportation—Entangled photon pair source (red circle) in ground station is used to teleport a qubit to the satellite. The unknown qubit, to be teleported, also comes from another entangled pair for technical reasons. See text for details [52]. (d) Entanglement distribution in downlink—Entangled photon pairs are distributed between two ground stations, separated by a record 1203 km on earth, by double downlink transmission [19].

gate and measurement needed for teleportation. Micius also distributed entanglement between two ground stations in China separated by 1203 km [19], as schematized in Fig. 2(d). Notably, they performed a Bell inequality test on the entangled pair, a measurement of non-locality and hence non-classicality, which increased the Bell test violation distance by almost an order of magnitude. Entanglement-based QKD was also achieved over 1,120 km in 2020 using this configuration [51]. Several so-called trusted-node QKD experiments were performed using Micius. In this scenario, the satellite acts as a trusted party and generates a unique key to be shared with each of the ground stations [54,122]. In one such experiment, a quantum-encrypted video call was conducted between Austria and China [54]. More recently, trusted-node QKD has been performed over 4600 km between two cities in China, with trusted nodes in both ground and satellite [122]. Launching a whole fleet of satellites to perform Global trusted node QKD has been considered [123]. Indeed, trusted nodes cannot distribute entanglement and hence cannot enable other functionalities of quantum internet like distributed quantum computing, sensing, or teleportation. To

accomplish them worldwide, along with completely secure QKD, global-scale entanglement distribution is needed. Trusted-node QKD using satellites have been viewed as more secure than using ground stations as trusted nodes because satellite nodes are remote in space. This may change with advances in space technology if access to space drastically improves.

After the success of the Micius satellite, several other satellite projects have been announced, initiated, or implemented. A smaller micro-satellite called Jinan-1 was launched in 2021 to perform QKD [124]. China is also considering launching more satellites soon, including higher-orbit satellites for more coverage [123]. A cubesat called SpooQy-1, developed by the National University of Singapore, tested an entangled source in orbit in 2019 [125]. Several countries are also working towards their own quantum satellite mission. Canada is preparing QEYSSat satellite and several optical ground stations [126,127]. European Union has initiated the SAGA (Security And crypto-GrAphic) mission [128,129] as part of its European Quantum Communications Infrastructure (EuroQCI), to integrate quantum security in its upcoming IRIS² satellite communication constellation. European Union is also developing Eagle-1 small satellite, being made with SES [130]. United States is testing quantum hardware with NASA's SEAQUE (Space Entanglement and Annealing QUantum Experiment) mission aboard International space station [131]. Indian Space Research Organisation (ISRO) announced development of a quantum satellite [132]. Private companies are also actively working towards developing quantum communications using satellites, including QuantumCTek in China (backed by the Micius satellite team), Boeing's quantum division, Spectral in Singapore, etc.

However, single LEO satellites cannot establish entanglement beyond $\sim 2000\text{--}3000$ km due to the curvature of earth. Higher-orbit satellites are one way to achieve this. Satellites in geostationary (GEO) orbit (at 36,000 km elevation) or even mid-earth orbits (MEO—orbits between LEO and GEO) can establish entanglement between two farther away places on earth. Diffraction loss will be very high, though for high orbits compared to LEO satellites. However, while LEO satellites have limited flyby times, higher orbits offer longer flyby times, with geostationary (GEO) satellites being effectively stationary relative to a ground station. This continuous availability increases the communication rate. However, even for this continuous coverage of two specific ground stations, GEO satellites are expected to have a very small rate of entanglement distribution (~ 1 Hz) [56]. Experiments have been performed using retroreflectors in higher Earth orbits to model the high-orbit transmission rates [114,133]. Even geostationary satellites cannot send photons to global distances (10,000–20,000 km, not even with 1 Hz rate), due to Earth's curvature and grazing incidence [56].

5. MEMORY-SATELLITE PROTOCOLS

Satellite schemes combined with quantum memories offer a way to achieve ultra-long distance (more than 10,000 km) distribution of entanglement. These could involve quantum repeaters over satellite chains or memories in single satellites.

5.1. Repeater Protocol with Satellites

The first such protocol was given in [56] (shown in Fig. 3(a)). Quantum non-demolition (QND) detectors are used for this protocol along with quantum memories. QND detectors detect

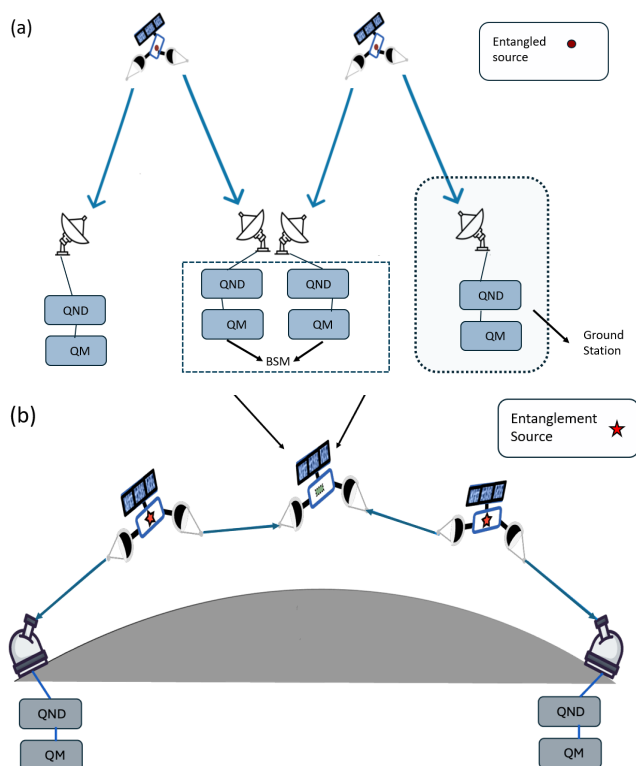


Fig. 3. Two repeater protocols over LEO satellites to distribute entanglement over global distances using quantum memories (QM) and quantum non-demolition (QND) detectors in ground stations [56]. In (a) the QM and QND detectors are kept in ground stations for operation advantages while in (b) the QM and QND detectors in the intermediate links (dashed box in (a)) are kept in the satellite to avoid extra intermediate ground link connections [57,58].

the presence of a photon without disturbing its quantum state [134–138]. Both QND detectors and memories are kept on the ground for the sake of easy operation and maintenance, while satellites will direct entangled photon pairs to the ground stations. The successfully transmitted entangled pairs are detected by QND detectors and subsequently stored in memories. Entanglement swapping between qubits stored in quantum memories is then performed, as shown in Fig. 3(a), using a projective measurement onto a Bell state. In [56] an equatorial satellite constellation was proposed. However, this method will work more generally for a constellation of satellites to distribute entanglement between any two points on earth.

Numerical simulations consider 4–8 links between the equatorial satellite chain, with the possibility of different orbital heights (500–1,500 km). Simulation parameters include 50 cm satellite transmitter diameters, 1 m ground telescope diameter, and 580 nm photon wavelength for the satellite-repeater transmission (motivated by Eu-doped yttrium orthosilicate memory storage wavelength). Efficiencies for sources, memory read and write operations, and single-photon detection are assumed to be 0.9. Efficiency for QND detectors is assumed to be 0.32. Also, repeater rates are explored in variation of these efficiencies. The numerical results (shown in Fig. 2 of [56]) demonstrate entanglement distribution rates per day as a function of total ground distance for direct transmission from high orbits and satellite repeaters. The rates for geostationary satellite direct transmission and repeaters are close around 4,000 km at about

$10^4 - 10^5$ qubits/day (~ 1 Hz). However, for longer distances (above 10,000 km) geostationary satellite rates fall off drastically, while satellite repeaters at 1,000–1,500 km orbits with 8 links still provide rates around 10^3 qubits per day at 20,000 km. The difference in rates also stems from considering a lower memory bandwidth for repeaters. Correspondingly, repeater calculations use a 10 MHz pair source repetition rate, while direct transmission uses 1 GHz. So, with higher memory bandwidth, repeater rates can be increased by two orders of magnitude. Moreover, frequency multiplexing has not been considered in [56] either for direct transmission or for satellite repeaters, which can increase rates further.

Quantum memories and QND detectors can alternatively be in satellites [57,58] (shown in Fig. 3(b)). Given recent atomic and optical physics experiments in space [139–141] and the development of transportable, standalone quantum memories [142], this possibility is becoming more plausible. QND and QM placed in a satellite would evade the extra downlink and atmospheric loss, multiple links simultaneously for successful entanglement transfer over a long distance, as well as potentially reduce the latency of the individual links. Space-based memories would entirely bypass the need for intermediate ground-space links, removing any dependence on weather conditions, except for the end links. This also obviates the need to place these terrestrial repeater stations in possibly inaccessible or inconveniently located areas (such as in the middle of an ocean). Coordination of the different link geometries is also simplified.

Simulations in [57] compare the space-based memory proposal with the earlier ground-based memory proposal [56]. The performance metric used is the total time to distribute entangled pairs. A total of 8 links corresponding to a repeater nesting level of 3 is assumed [34]. Other parameters include beam divergence of $4 \mu\text{rad}$, total memory efficiency, and QND detector efficiency of 0.9 while a source rate of 20 MHz. Numerical results presented in Fig. 2 of [57] demonstrate three orders of magnitude higher entanglement distribution rate using space-based memory-QND system than ground-based memory-QND. This also translates to significantly lower memory storage time requirements. Variation of repeater rates with different beam divergence values (ranging from 1 to $10 \mu\text{rad}$), and memory efficiency (ranging from 0.5 to 1) is shown. More recent studies have shown that memory optimization can increase rates even further [143]. A recent proposal involving single atom systems—both as single photon sources and memories—showed their architecture lowers the required multiplexed capacity [144]. Note that these protocols could be applied to conventional ground-based repeater schemes and there have been other conventional repeater proposals that use QND [145].

5.2. Memories in Single Satellites

Multiple other architectures are possible using memories and satellites. One such proposal, as described in Fig. 4(a), consists of a putting a very long-term memory (storage time in minutes) in a satellite which also contains an entangled source [146]. One photon of the entangled pair is transmitted downlink while the other is stored in the memory. If the photon is not received at the ground station, one would flush the memory qubit and try to store a photon in the same qubit again. When the photon is received successfully at the ground station, the qubit will be kept in memory. Now, the next photon can be stored in the next memory qubit and that is how all the memory capacity can be used.

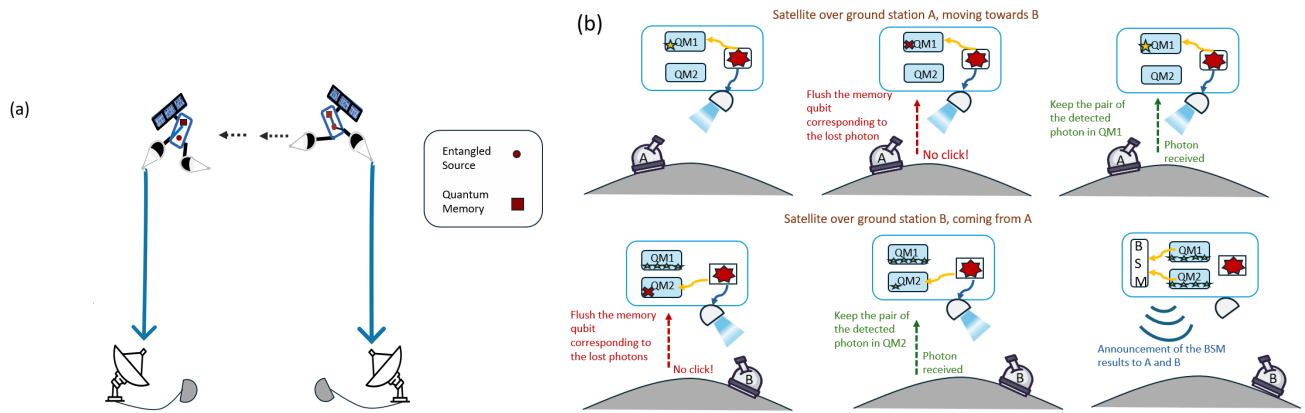


Fig. 4. Entanglement is distributed using very long storage-time memory in a single satellite. (a) One Photon of an entangled pair is stored in the memory (red Square) which is later retrieved and transmitted downlink once the satellite has physically moved to a far-away destination [1, 146]. (b) Rates of the single-satellite protocol can be dramatically improved by using a time-delayed repeater protocol using two memories that result in complete usage of the memory multiplexing capacity [59].

The satellite then physically moves from one place to another physically and when it reaches the destination, the stored photon is retrieved and sent downlink. This protocol would require a very long storage time memory with storage time at least in minutes, preferably in order of an hour as the satellite needs to physically move over a large distance for this to be useful. In this context, rare-earth ion based solid state system has been shown to have coherence times as large as 6 hours [147]. More recently, the same system has been engineered to show several improvements including coherence times exceeding 10-hours [148]. A functioning memory demonstration with more than 1 hour storage time using atomic-frequency combs has also been performed [75], although with storage of classical bright pulses.

The long storage time memory also must have high multimode capacity through spatial, temporal, or frequency multiplexing for effective transmission rate for several reasons. One is simply that there is a large time delay due to the physical movement of the low-earth orbit satellite to long distances (~ 20 minutes for around 10,000 km). Considering this time delay in transmission, successfully transferring only a few qubits worth of quantum information in a single journey would result in very low transmission rates. Hence, large multiplexing capability is necessary, which can be attained in principle with atomic frequency comb memories with long storage time [75, 79, 149].

Another important reason for large multiplexing is the loss at each ground link, including the effect of memory efficiency. Consider, for example, links with 20 dB loss including memory efficiency, and a memory with 10,000 multiplexing capacity. The first link would be able to fill up the satellite memory, as described previously, with a modest entangled pair generation rate. However, on the second link, only 100 e-bits will be successfully transferred to the ground station. This will mean a very low transmission rate and a huge loss of memory capacity.

To solve the above problem, a time-delayed repeater protocol with double quantum memory has recently been invented [59], as shown in Fig. 4(b). One photon of an entangled pair is stored, and another is sent down at the ground station just like before, filling up the memory on the satellite. Then the satellite can fly to its destination station and do the exact same thing using another memory (QM2 in Fig. 4(b)). Then, when all the memory qubits in the other memory are entangled

with the second ground station, we can perform entanglement swapping by Bell-state measurements (or C-NOT gates and direct measurements if that can be arranged in the satellite). Such a time-delayed repeater with a single satellite and two memories would result in proper use of the maximum quantum memory capacity and hence increase entanglement distribution or QKD rates by several orders of magnitude [59]. Furthermore, it significantly increases the maximum tolerable loss over its single-memory counterpart [146] when the finite key effects are taken into account.

The protocol uses an entangled photon pair source with a rate of 5 MHz and considers a transmission period of 240 seconds. The analysis includes a memory noise probability of 10^{-3} , a background count probability of 6.4×10^{-7} , and a detector dark count probability of 10^{-7} , within a 200 ns temporal window. Memory efficiency is set to 0.6, and detector efficiency to 0.8. These simulation parameters are chosen for illustrative purposes and can be adjusted to explore different scenarios. The calculations determine the finite key length and secure key rate as a function of average single-channel loss and memory dephasing. Results demonstrate that the double memory protocol achieves orders of magnitude higher secure key rates and tolerates greater channel losses than a single memory scheme. For example, with ideal quantum memories, the double memory scheme tolerates channel losses up to 42 dB, a significant improvement over the single memory scheme's limit of 28 dB.

These developments also sparked a complementary line of research: beyond mitigating transmission losses, could the space environment itself enhance the performance of quantum memories? In particular, recent proposals suggest that Bose-Einstein condensate (BEC)-based quantum memories could benefit substantially from microgravity conditions, achieving coherence times and operational stability that surpass their terrestrial counterparts by orders of magnitude [150]. Such findings open new avenues for leveraging space not only as a transmission channel, but also as an active medium for advancing quantum technologies.

6. SATELLITE-RELAY: JUST REFLECT

A conceptually and technologically simpler approach to achieve global-scale quantum communications has recently been put forward [60]. This protocol uses a satellite chain to simply re-

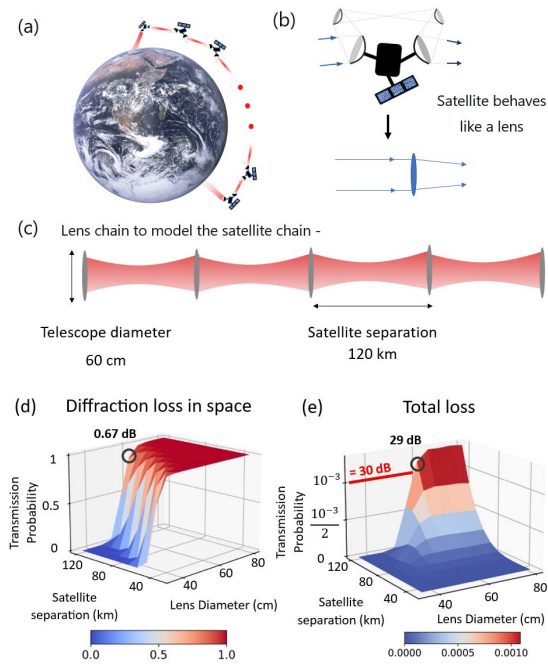


Fig. 5. The satellite relay architecture of [60] is shown, for global-scale quantum communication without quantum memory or quantum repeaters. (a) Photons are sent from one side of the globe to another by being reflected from one satellite to another and being guided along the surface of the earth (satellite separation exaggerated). (b) Each satellite has telescopes with curved mirrors that together focuses the light, while also bending it in the direction of the next satellite. Effectively the whole telescope mirror assembly in each satellite behaves like one lens (as shown, without considering the light bending that can't be modeled by a lens). (c) The chain of satellites behave like a set of lenses and contain light beam divergence or diffraction loss indefinitely over very long distance. (d), (e) Simulation results reproduced from [60] shows diffraction loss in the space segment (without ground links) in (d) and total loss in (e), both for entanglement distribution at 20,000 km. For our chosen parameter values (shown in black circle), diffraction loss is nearly eliminated even at 20,000 km (0.67 dB only), while total loss is contained below 30 dB. Parameter values are satellite telescope diameter of 60 cm, satellite separation of 120 km, 2% reflection loss at each satellite and 500 km orbits [60]. See text for more details.

flect entangled photons and, crucially, does not require quantum memories or repeater protocols; see Fig. 5(a). A chain of satellites in LEO acts as a long-distance optical relay and thereby permits communication without trusted nodes and entanglement distribution. Each satellite uses telescope mirrors to re-focus the light like a lens to compensate the light divergence so that the beam can be accommodated by the next satellite. The satellites inside the chain move together in the same orbit, greatly simplifying satellite tracking and suppressing channel loss due to pointing errors. The chain of satellites in Earth's orbit is described as effectively behaving like a set of lenses on an optical bench, confining photonic qubits faithfully over large distances [60].

6.1. Low Loss over Global Distances

The proposed architecture, termed All-Satellite Quantum Network (ASQN) in [60], minimizes photon loss over long distances in four principal ways.

1. Elimination of Diffraction Loss Using Curved Satellite Mirrors: Diffraction loss in ASQN is effectively eliminated in the satellite chain through continuous focusing at each satellite. The curved telescopes at each satellite create an effective “satellite lens” to re-focus light. A four-mirror telescope assembly is shown in Fig. 5(b), which can focus input light like a lens, effectively turning the whole satellite into a lens. The chain of satellites, modeled by the set of lenses, mitigates diffraction over long distance as illustrated in Fig. 5(c).

Detailed simulation of light propagation has been carried out in [60] for different parameter values, different scenarios, and different forms of errors to show the feasibility and robustness of ASQN protocol. Figures 5(d) and 5(e) show reproduced simulation results (Figs. 3(b) and 7(c) in [60]). Entangled pair transmission probability is simulated for different satellite separations and lens (telescope) diameter values at 20,000 km, in both cases. Only diffraction loss in the space links (without considering ground links or errors) is shown in Fig. 5(d), while Fig. 5(e) shows total loss including diffraction loss with ground link, reflection loss, atmospheric attenuation, effect of errors, etc. Diffraction loss is simulated numerically by propagating the beam from one lens to the next, providing a thin lens phase shift at each lens, and then using an aperture to truncate the beam according to the lens size. Simulations in Fig. 5(d) confirm the near-complete elimination of diffraction loss (only 0.67 dB) even at global distances of 20,000 km—for lens (satellite) separation of $L_0 = 120$ km, lens (telescope) diameter of $d = 60$ cm and $\lambda = 800$ nm wavelength (shown in black circle). Beam size at the satellite (w_0) is chosen as 17.48 cm, so that $L_0 = \text{Rayleigh range} = \frac{\pi w_0^2}{\lambda}$. “Satellite Lens” focal length (of 60 km) is chosen to focus the divergent beam exactly at the midpoint (at 60 km) between two satellites, considering focal shift [151,152]. Smaller wavelengths (λ) can afford us larger satellite separations (L_0) resulting in less number of satellites, but atmospheric attenuation and reflectivity values also need to be considered for an optimal wavelength choice. Diffraction loss has been found to be robust against the effect of lens (satellite) position errors and focal length errors as well [60], as discussed later in this section. This indirectly verified the effects of different satellite motions which isn't simulated directly as a stationary set of lenses is considered. Apart from focusing, the telescope mirrors slightly bend the light beam to the next satellite, eventually directing it along the Earth's curvature.

2. Only Reflection at Each Satellite: Loss at each satellite (e.g., component absorption loss) is the only exponentially scaling loss in ASQN. It is minimized by only allowing mirrors in the light path, at least in most satellites, because of the inherently low loss in mirrors. If the two large mirrors are metal mirrors with as much as 1% reflectivity loss, there would be a reasonable 15 dB total reflection loss at 20,000 km. If smaller front mirrors are present (like in Fig. 5(b)), they can be ultra-high reflectivity Bragg mirrors with negligible loss ($< 0.0001\%$). If Bragg mirrors can be used for the two larger mirrors as well [153], even the mirror loss can be completely eliminated. Refraction loss significantly impacts total loss scaling, rising rapidly with a larger number of satellites—leading to high loss for smaller satellite separations (see Fig. 5(e)), irrespective of telescope sizes.

3. Synchronous Orbits Minimize Tracking: Tracking error is also nearly absent within the satellite chain in ASQN because satellites inside the chain are co-moving in the same

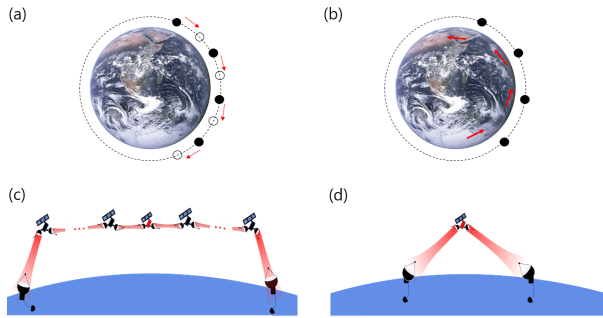


Fig. 6. Satellite tracking loss in ASQN [60] is nearly eliminated within the satellite chain as shown in (a) and (b). (a) The Satellite chain moves synchronously (in the direction of red arrows). The filled and empty circles show the initial and later position of the satellites. (b) In the reference frame of one satellite—all other satellites are stationary and the Earth moves below. So, almost no dynamic tracking (i.e., pointing or point-ahead) is needed within the satellite chain, except due to errors in satellite positioning. The satellites only need to be aligned for transmission along the chain. (c) and (d) Ground link loss is much less in satellite-relay compared to single satellite transmission. (c) The chain of satellites enables near-vertical transmission to ground, while a more oblique incidence is necessary in for single satellites as shown in (d).

orbit (Fig. 6(a)). Hence, the satellites are stationary relative to each other in their frame of reference, as depicted in Fig. 6(b). Thus, mostly just light alignment is necessary in the chain along with very small residual tracking for orbital deviations and other errors. Tracking is only required at the up- and downlinks or between independent satellite chains in different orbits, as discussed in the next section.

4. Vertical Ground Link: The preceding discussion focused on minimizing losses within the satellite chain, which constitutes the longest distances in the communication channel. Indeed, ASQN also involves ground-to-satellite and satellite-to-ground links like all other satellite protocols, which experience diffraction, attenuation, and turbulence losses. However, ASQN utilizes near-vertical ground transmission links, reducing losses associated with grazing or oblique incidence commonly encountered in a single LEO satellite as shown in Fig. 6(c). Hence, diffraction and atmospheric losses associated with ground link transmission in ASQN (even for a 20,000 km transmission) will be significantly less than that of a single satellite like Micius, as depicted in Fig. 6(d), if a similar-sized telescope and the same elevation are considered. Total diffraction loss including ground link is only 5 dB in ASQN as 60 cm telescopes and vertical links are used. Satellites are assumed to be at 500 km orbit with 1.2 m receiving telescopes in the ground (assumed for Fig. 5(e) as well). Hence, in ASQN photon loss is low both in short and long distances, compared to other protocols involving oblique satellite transmission.

Considering all the above factors and further losses like that from atmospheric attenuation, as well as the effect of errors, the total loss for entanglement distribution is contained below 30 dB in ASQN (~ 29 dB, as shown in black circle in Fig. 5(e))—for 20,000 km optical path length inside the satellite chain. Hence, a 1 GHz source would enable a 1 MHz entanglement distribution rate even at 20,000 km. This calculation assumed a satellite-based source, 60 cm-diameter satellite telescopes, 120 km satellite separations, 2% reflection loss at each satellite, and 500 km orbits. Effect of errors on diffraction showed a 12 km (10%) er-

ror in satellite separation, 0.6 cm (2%) error in telescope lateral position, and 3 km (5%) in focal length error contribute to only around 5.7 dB extra diffraction loss at 20,000 km. This directly verify robustness against focusing errors and indirectly verify effects of satellite motion and orbital deviations inside the satellite chain that leads to residual tracking requirements, as explained in [60]. The different factors of loss, in entanglement distribution from a satellite-based source, are summarized in the following table (for parameters mentioned earlier in the text).

Loss Due to Different Factors (Approximate)	
Diffraction loss within the satellite chain	0.67 dB
Total diffraction loss including ground link	5 dB
Reflection loss (2% at each satellite)	15 dB
Other losses—atmospheric attenuation and loss due to errors and inefficiencies	10 dB
Total entanglement distribution loss at 20,000 km	30 dB

6.2. Background and Protocols

As mentioned, satellite chains for trusted-node QKD have been proposed [103,123]. Also, some optical relay designs have been proposed before for quantum communication using drones and satellites [154,155]. However, only high-orbit reflectors were considered for satellites, which led to a high degree of diffraction for photons because of the large distances covered through high orbits and no focusing of light. Nevertheless, this approach requires only a few reflectors and allows a wide area of collection. We note that several experiments have been performed using retro-reflectors in high orbits like geo-stationary orbits, to experimentally ascertain channel loss [116,119,133,156]. ASQN differs from previous high-orbit studies in that its telescope mirror assemblies mitigate enormous diffraction loss through continuous focusing while being in low orbit limits ground link loss, allowing the distribution of quantum-level light signals over very long distances.

There has been a consistent effort in creating inter-satellite laser links for classical communication [157–159]. In these implementations, however, all the satellites are moving at high speeds with respect to each other and the satellites are generally not equipped with large telescopes, since light is just detected at the next satellite and classical ground link rely on radio frequency communication. Recently, nearly continuous inter-satellite laser links with more 100 GB/s capacity has been achieved with more than 5000 satellites by the Starlink internet service [67,68].

ASQN can accommodate different quantum communication protocol. Till now, we discussed the entanglement distribution with the entanglement source on a satellite, sending photons down to the Earth via two downlinks. Another protocol, termed as “Qubit Transmission” was proposed in ASQN. It is a prepare and measure scheme where weak laser pulses are sent in one way transmission from a ground source to a ground detector through the satellite-relay. This scheme can perform QKD using the BB84 protocol [2]. Placing both the source and detector on the ground offers significant advantages in terms of space, energy, access to advanced technologies like cryogenics, and qubit multiplexing capabilities. Most importantly, both the source and detector can be changed to create different protocols and experimentation.

Qubit transmission will have one uplink and one downlink transmission, facing uplink atmospheric turbulence. Uplink turbulence distorts, fragments, and enlarges the beam, and only a small portion of the beam is caught in the first satellite. However, after the uplink to satellite—ASQN's satellite lenses effectively control further spread of beam divergence along the chain from the distorted beam (see Fig. 6 of [60]). Simulations using multiple phase screens [60,160] confirmed that diffraction loss is limited after the first uplink. Though the distorted beam contains different order modes of light, the lens systems confine fundamental/low-order modes, ensuring only 2 dB ($\sim 35\%$) extra diffraction loss at 20,000 km (negligible compared to the initial 22 dB uplink loss at 500 km orbit). This can be understood as the distorted beam containing 35% higher order modes that can't be confined. The impact of transmitting the distorted beam is seen indirectly, though, in requiring closer satellite separation of 80 km in the simulation—instead of the 120 km separation needed for entanglement distribution (without uplink).

In ASQN, worldwide coverage can be enabled using nearly orthogonal satellite chains covering the entire globe. The bulk of the transmission will be along the satellite chains, where satellite tracking will be minimal due to synchronous orbits. However, to connect two arbitrary points, one connection between two separate chains will be necessary where dynamic satellite tracking will be needed. Such tracking has already been achieved in classical satellite-to-satellite links [67,68]. If a worldwide network is constructed, any point on the ground should always have one (ideally multiple) satellite in its view. Hence, the network in ASQN will not be limited by satellite flyby time. As one satellite passes further, one can always point at the next satellite and establish nearly continuous quantum communication. Beyond flyby, the use of multiple chains will allow optimizing the network capacity, which is an open research question in quantum communication. This question has been very recently explored for ASQN connected with ground-based fiber networks [161].

6.3. Challenges

Along with introducing the protocol, a feasibility study of ASQN has been conducted in [60], exploring various aspects such as the use of vortex beams for on-axis telescope setups, alignment, and tracking procedures, the effects of space on mirror performance, different forms of wavefront aberration, different qubit types, and focal length adjustments for the satellite lenses. There are, of course, more effects to analyze like temperature dependence, source etendue effect [162,163], detailed simulation of satellite motion, and acquiring, pointing, and tracking (APT) process, possible small effects in optical near-field, and more such detailed engineering concerns. The recent rapid progress in space industry [62,63,67–70] provides the backbone to launch (possibly even affordably soon) a large network of satellites required for ASQN, in which one chain spanning 20,000 km will itself require about 160 ($\sim 20,000/120$) satellites. Overall, a comprehensive diffraction analysis demonstrated the effectiveness and robustness of ASQN showing the practicality of a satellite-relay while acknowledging the engineering challenges associated with building and deploying such a network, particularly wavefront aberration control in mirror surface design and residual satellite tracking requirements over the long chain.

6.4. Ground-Based Relay: Vacuum Beam Guides

A similar, but ground-based, relay proposal has recently emerged [50], using a series of lenses within vacuum tubes. These are actual lenses, in contrast to the mirror setup working as an effective lens in ASQN. The lenses periodically focus light to transmit quantum information over a long distance. This approach, termed vacuum beam guides, directly employs lenses spaced 4 km apart inside vacuum tubes, and is partially inspired by Laser Interferometer Gravitational-Wave Observatory (LIGO) infrastructure [164]. Numerical modeling considered loss due to scattering from lenses, absorption loss from residual gas in the vacuum tube, and lens alignment errors—promising only 10^{-4} dB/km loss. This proposal avoids dealing with atmospheric up- and down-links, in contrast to satellites in ASQN.

However, vacuum beam guides have their own challenges. For instance, lenses cannot bend light passing through their center, and additional optical elements like mirrors or prisms (with additional losses) would be necessary to accommodate the Earth's curvature. However, mirror assemblies like those that used in ASQN [60] can mitigate this. One other issue is lens vibration from ground, which was taken into account in simulations, but can vary depending on the local environment. Focal length fluctuation of the large (4 km) focal length lenses due to thermal variations is another concern. A broader and more important issue concerns the practicalities of constructing and maintaining the numerous vacuum beam guides for world-wide communications, including taking into account the varying geography and terrains as well as political and environmental considerations. In contrast, satellites are much more established, including their manufacturing and operation as well as legal and political considerations. However, given there is no practical solution to achieve long-distance quantum communication currently—all avenues and ideas should be pursued enthusiastically until a clear winner is established.

7. COMBINATION OF SATELLITE-RELAY AND QUANTUM MEMORIES

Quantum memories will likely be required in quantum networks to achieve advanced functionalities [6]. Some of the stringent requirements on memory performance, such as efficiency and multiplexing capacity, that are required for conventional ground-based repeaters or other memory-satellite proposals can be relaxed, though, due to satellite-relay's elimination of diffraction loss [60]. Especially, memory efficiency will not be a big factor as only a few memories (e.g., two) are needed. Multiplexing capacity needed will also be more relaxed. The primary reasons for incorporating quantum memories for quantum networks are due to heralding and causality as well as further loss avoidance. Quantum memories store entangled photons while waiting for a classical signal that indicates which specific entangled qubit has been heralded to another location in multiplexed communications (heralding) or what the outcome of a measurement was on an entangled qubit at a distant location (causality). Several operations, like quantum teleportation, require quantum operations that are conditioned on the results of previously performed measurements due to causality. Loss reduction due to repeaters is especially relevant for uplink transmission. For downlink entanglement distribution rates can be increased much further too by using satellite repeaters nodes in combination with the relay. In the space-based satellite relay, loss in inter-satellite links of

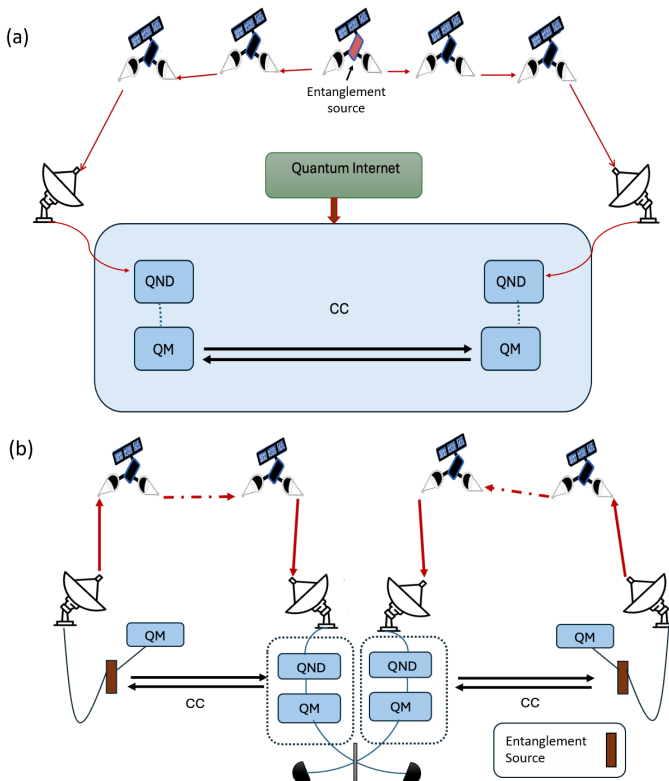


Fig. 7. Combination of satellite-relay and quantum memories. (a) Only two Quantum memories (QM) can be incorporated only at the end to create quantum internet capabilities in satellite-relay architecture of ASQN [60]. However, that will require Quantum non-demolition (QND) detectors. (b) Repeater over relay—with two detectors at the middle, QND detectors are not essential anymore. Quantum internet capabilities are achieved with higher rates. Note that the QM and QND in the middle are optional to increase rates.

2,000 km is more than 15 dB [57]. Using multiple relay nodes inside each inter-satellite link will decrease the loss drastically. For example, 2,000 km space transmission loss in ASQN is less than 2 dB with about 0.1 dB diffraction loss and 1.5 dB reflection loss. A relay-repeater combination with such low loss links can achieve higher entanglement distribution rates than what both relay and repeaters can achieve individually. However, to achieve very high rates, large multiplexing capabilities (time or frequency) will be needed for quantum memories along with long storage time [60].

Different strategies for incorporating quantum memories into ASQN have been proposed (see Fig. 7) [60]. For instance, QND can identify and quantum memories can store photons distributed by ASQN, e.g., for interfacing with a ground-based networks, quantum computers, or sensors (see Fig. 7(a)). Alternatively, a repeater protocol (with or without QND) can be performed using ground-based entangled sources but replacing the terrestrial channels with space transmission (Fig. 7(b)). Clearly, there are open research questions how satellite-relays can be used in conjunction with memories, repeater protocols, and other forthcoming quantum technologies.

Importantly, the above schemes emphasize the flexibility of satellite-relay in accommodating both relay and repeater functionalities. While relay's primary advantage lies in eliminating the need for quantum memories in the initial stages of building a global quantum network, it can be seamlessly integrated

with quantum repeaters when necessary. This hybrid approach allows for a staged development of the quantum internet, starting with simpler functionalities and gradually incorporating more complex ones as quantum memory technology matures.

8. CONCLUSION

Global quantum communication networks face the formidable challenge of transmitting quantum information over long, lossy, channels. While ground-based quantum repeaters offer a potential solution, their reliance on high-performance quantum memories remains a significant hurdle. Satellite-based approaches, exemplified by the Micius satellite achieving entanglement distribution over 1,200 km, have demonstrated remarkable success in overcoming loss limitations. In the tailwinds of this demonstration, we reviewed several long-distance quantum communication proposals using satellites: either with satellite-based repeaters, satellites equipped with long-lived quantum memories, or satellite-relay protocols, where photons are reflected from one satellite to another. Such approaches benefit from the rapid progress in the space industry, including the advent of rapidly reusable mega-rockets [61–63] and deployment of large-scale classical-internet satellite constellations reducing launch costs [67–70]. The eventual architecture for a quantum internet may even be a combination of different approaches, whether its goal is to achieve global-scale QKD, diverse networked quantum technologies building towards a quantum internet, to realize fundamental science, or beyond.

Acknowledgment. Authors acknowledges Aephraim M. Steinberg for fruitful discussions. M.M. and J.R.L. acknowledge support from Boeing. J.S.S. and D.K.L.O. would like to acknowledge the support of the EPSRC Quantum Technology Hub in Quantum Communications (EP/T001011/1). This work was supported by the EPSRC International Network in Space Quantum Technologies INSQT (EP/W027011/1). D.K.L.O. is supported by the EPSRC Integrated Quantum Networks Hub (EP/Z533208/1). M.K. and M.G. acknowledge the support from the DLR through funds provided by the Federal Ministry for Economic Affairs and Climate Action (Bundesministerium für Wirtschaft und Klimaschutz, BMWK) under Grants No. 50WM1958, 50WM2055 and 50WM2347. M.G. further acknowledges funding from the European Union's Horizon 2020 research and innovation programme under the Marie Skłodowska-Curie grant agreement No. 894590 and Einstein Foundation Berlin for support. Y.C.C. and H.H.J. acknowledge support from the National Science and Technology Council (NSTC), Taiwan, under the Grants Nos. 112-2112-M-001-079-MY3 and NSTC-112-2119-M-001-007, from Academia Sinica under Grant AS-CDA-113-M04 and are also grateful for support from TG 1.2 of NCTS at NTU. C.S. acknowledges the Natural Sciences and Engineering Research Council of Canada for its Alliance Quantum Consortia grants ARAQNE and QUINT, and the National Research Council for its High-Throughput Secure Networks challenge program.

Disclosures. The authors declare no conflicts of interest.

Data availability. No data were generated or analyzed for the present article. All results and graphs were reproduced from previously published research articles, which were duly cited.

REFERENCES

1. C. Simon, "Towards a global quantum network," *Nat. Photon.* **11**, 678–680 (2017).
2. C. H. Bennett and G. Brassard, "Quantum cryptography: public key distribution and coin tossing," in *IEEE International Conference on Computers, Systems, and Signal Processing*, Bangalore, December 1984, pp. 175–179.

3. A. K. Ekert, "Quantum cryptography based on Bell's theorem," *Phys. Rev. Lett.* **67**, 661–663 (1991).
4. C. H. Bennett, G. Brassard, and N. D. Mermin, "Quantum cryptography without Bell's theorem," *Phys. Rev. Lett.* **68**, 557–559 (1992).
5. F. Xu, X. Ma, Q. Zhang, *et al.*, "Secure quantum key distribution with realistic devices," *Rev. Mod. Phys.* **92**, 025002 (2020).
6. S. Wehner, D. Elkouss, and R. Hanson, "Quantum internet: a vision for the road ahead," *Science* **362**, eaam9288 (2018).
7. H. J. Kimble, "The quantum internet," *Nature* **453**, 1023–1030 (2008).
8. D. Gottesman, T. Jennewein, and S. Croke, "Longer-baseline telescopes using quantum repeaters," *Phys. Rev. Lett.* **109**, 070503 (2012).
9. P. Kómár, E. M. Kessler, M. Bishof, *et al.*, "A quantum network of clocks," *Nat. Phys.* **10**, 582–587 (2014).
10. D. Main, P. Drmota, D. Nadlinger, *et al.*, "Distributed quantum computing across an optical network link," *Nature* **638**, 383–388 (2025).
11. H. Aghaee Rad, T. Ainsworth, R. Alexander, *et al.*, "Scaling and networking a modular photonic quantum computer," *Nature* **638**, 912–919 (2025).
12. J. Liu, T. Le, T. Ji, *et al.*, "The road to quantum internet: Progress in quantum network testbeds and major demonstrations," *Prog. Quantum Electron.*, **99**, 100551 (2024).
13. A. Broadbent, J. Fitzsimons, and E. Kashefi, "Universal blind quantum computation," in *2009 50th Annual IEEE Symposium on Foundations of Computer Science*, (IEEE, 2009), pp. 517–526.
14. P. Arrighi and L. Salvail, "Blind quantum computation," *Int. J. Quantum Inf.* **4**, 883 (2006).
15. S. Barz, E. Kashefi, A. Broadbent, *et al.*, "Demonstration of blind quantum computing," *Science* **335**, 303–308 (2012).
16. V. Giovannetti, S. Lloyd, and L. Maccone, "Quantum private queries," *Phys. Rev. Lett.* **100**, 230502 (2008).
17. M. Jakobi, C. Simon, N. Gisin, *et al.*, "Practical private database queries based on a quantum-key-distribution protocol," *Phys. Rev. A At. Mol. Opt. Phys.* **83**, 022301 (2011).
18. M. Hillery, V. Bužek, and A. Berthiaume, "Quantum secret sharing," *Phys. Rev. A* **59**, 1829–1834 (1999).
19. J. Yin, Y. Cao, Y.-H. Li, *et al.*, "Satellite-based entanglement distribution over 1200 kilometers," *Science* **356**, 1140–1144 (2017).
20. B. Hensen, H. Bernien, A. E. Dréau, *et al.*, "Loophole-free Bell inequality violation using electron spins separated by 1.3 kilometres," *Nature* **526**, 682–686 (2015).
21. P. Xu, Y. Ma, J.-G. Ren, *et al.*, "Satellite testing of a gravitationally induced quantum decoherence model," *Science* **366**, 132–135 (2019).
22. R. Barzel, M. Gündoğan, M. Krutzik, *et al.*, "Entanglement dynamics of photon pairs and quantum memories in the gravitational field of the earth," *Quantum* **8**, 1273 (2024).
23. J. Borregaard and I. Pikovski, "Testing quantum theory on curved space-time with quantum networks," *arXiv*, *arXiv* (2024).
24. D. Rideout, T. Jennewein, G. Amelino-Camelia, *et al.*, "Fundamental quantum optics experiments conceivable with satellites—reaching relativistic distances and velocities," *Class. Quantum Gravity* **29**, 224011 (2012).
25. M. Mohageg, L. Mazzarella, C. Anastopoulos, *et al.*, "The deep space quantum link: prospective fundamental physics experiments using long-baseline quantum optics," *EPJ Quantum Technol.* **9**, 25 (2022).
26. W. K. Wootters and W. H. Zurek, "A single quantum cannot be cloned," *Nature* **299**, 802–803 (1982).
27. D. Dieks, "Communication by EPR devices," *Phys. Lett. A* **92**, 271 (1982).
28. S. Ghosh, G. Kar, and A. Roy, "Local cloning of Bell states and distillable entanglement," *Phys. Rev. A At. Mol. Opt. Phys.* **69**, 052312 (2004).
29. R. Ursin, F. Tiefenbacher, T. Schmitt-Manderbach, *et al.*, "Entanglement-based quantum communication over 144 km," *Nat. Phys.* **3**, 481–486 (2007).
30. A. Boaron, G. Boso, D. Rusca, *et al.*, "Secure quantum key distribution over 421 km of optical fiber," *Phys. Rev. Lett.* **121**, 190502 (2018).
31. T. Schmitt-Manderbach, H. Weier, M. Fürst, *et al.*, "Experimental demonstration of free-space decoy-state quantum key distribution over 144 km," *Phys. Rev. Lett.* **98**, 010504 (2007).
32. H.-J. Briegel, W. Dür, J. I. Cirac, *et al.*, "Quantum repeaters: the role of imperfect local operations in quantum communication," *Phys. Rev. Lett.* **81**, 5932–5935 (1998).
33. N. Sangouard, C. Simon, H. de Riedmatten, *et al.*, "Quantum repeaters based on atomic ensembles and linear optics," *Rev. Mod. Phys.* **83**, 33–80 (2011).
34. L.-M. Duan, M. D. Lukin, J. I. Cirac, *et al.*, "Long-distance quantum communication with atomic ensembles and linear optics," *Nature* **414**, 413–418 (2001).
35. M. K. Bhaskar, R. Riedinger, B. Machielse, *et al.*, "Experimental demonstration of memory-enhanced quantum communication," *Nature* **580**, 60–64 (2020).
36. M. Lucamarini, Z. L. Yuan, J. F. Dynes, *et al.*, "Overcoming the rate-distance limit of quantum key distribution without quantum repeaters," *Nature* **557**, 400–403 (2018).
37. Y.-F. Pu, S. Zhang, Y.-K. Wu, *et al.*, "Experimental demonstration of memory-enhanced scaling for entanglement connection of quantum repeater segments," *Nat. Photon.* **15**, 374–378 (2021).
38. C. Knaut, A. Suleymanzade, Y.-C. Wei, *et al.*, "Entanglement of nanophotonic quantum memory nodes in a telecom network," *Nature* **629**, 573–578 (2024).
39. V. Krutyanskiy, M. Canteri, M. Meraner, *et al.*, "Telecom-wavelength quantum repeater node based on a trapped-ion processor," *Phys. Rev. Lett.* **130**, 213601 (2023).
40. L. Jiang, J. M. Taylor, K. Nemoto, *et al.*, "Quantum repeater with encoding," *Phys. Rev. A At. Mol. Opt. Phys.* **79**, 032325 (2009).
41. M. Zwerger, A. Pirker, V. Dunjko, *et al.*, "Long-range big quantum-data transmission," *Phys. Rev. Lett.* **120**, 030503 (2018).
42. W. Munro, K. Harrison, A. Stephens, *et al.*, "From quantum multiplexing to high-performance quantum networking," *Nat. Photon.* **4**, 792–796 (2010).
43. S. Muralidharan, L. Li, J. Kim, *et al.*, "Optimal architectures for long distance quantum communication," *Sci. Rep.* **6**, 20463 (2016).
44. K. Azuma, K. Tamaki, and H.-K. Lo, "All-photonic quantum repeaters," *Nat. Commun.* **6**, 6787 (2015).
45. W. J. Munro, A. M. Stephens, S. J. Devitt, *et al.*, "Quantum communication without the necessity of quantum memories," *Nat. Photon.* **6**, 777–781 (2012).
46. S. Muralidharan, J. Kim, N. Lütkenhaus, *et al.*, "Ultrafast and fault-tolerant quantum communication across long distances," *Phys. Rev. Lett.* **112**, 250501 (2014).
47. J. Borregaard, H. Pichler, T. Schröder, *et al.*, "One-way quantum repeater based on near-deterministic photon-emitter interfaces," *Phys. Rev. X* **10**, 021071 (2020).
48. M. Pant, H. Krovi, D. Englund, *et al.*, "Rate–distance tradeoff and resource costs for all-optical quantum repeaters," *Phys. Rev. A* **95**, 012304 (2017).
49. I. Cozmuta, S. Cozic, M. Poulain, *et al.*, "Breaking the silica ceiling: Zblan-based opportunities for photonics applications," *Proc. SPIE* **11276**, 133–147 (2020).
50. Y. Huang, F. Salces-Carcoba, R. X. Adhikari, *et al.*, "Vacuum beam guide for large scale quantum networks," *Phys. Rev. Lett.* **133**, 020801 (2024).
51. J. Yin, Y.-H. Li, S.-K. Liao, *et al.*, "Entanglement-based secure quantum cryptography over 1,120 kilometres," *Nature* **582**, 501–505 (2020).
52. J.-G. Ren, P. Xu, H.-L. Yong, *et al.*, "Ground-to-satellite quantum teleportation," *Nature* **549**, 70–73 (2017).
53. S.-K. Liao, W.-Q. Cai, W.-Y. Liu, *et al.*, "Satellite-to-ground quantum key distribution," *Nature* **549**, 43–47 (2017).

54. S.-K. Liao, W.-Q. Cai, J. Handsteiner, *et al.*, "Satellite-relayed intercontinental quantum network," *Phys. Rev. Lett.* **120**, 030501 (2018).
55. S. K. Gagliardi and M. Robert, *Satellite Communications* (John Wiley & Sons, 1995).
56. K. Boone, J.-P. Bourgoin, E. Meyer-Scott, *et al.*, "Entanglement over global distances via quantum repeaters with satellite links," *Phys. Rev. A* **91**, 052325 (2015).
57. M. Gündoğan, J. S. Sidhu, V. Henderson, *et al.*, "Proposal for space-borne quantum memories for global quantum networking," *NPJ Quantum Inf.* **7**, 128 (2021).
58. C. Liorni, H. Kampermann, and D. Bruß, "Quantum repeaters in space," *New J. Phys.* **23**, 053021 (2021).
59. M. Gündoğan, J. S. Sidhu, M. Krutzik, *et al.*, "Time-delayed single satellite quantum repeater node for global quantum communications," *Opt. Quantum* **2**, 140 (2024).
60. S. Goswami and S. Dhara, "Satellite-relayed global quantum communication without quantum memory," *Phys. Rev. Appl.* **20**, 024048 (2023).
61. M. Elvis, C. Lawrence, and S. Seager, "Accelerating astrophysics with the SpaceX starship," *Phys. Today* **76**, 40–45 (2023).
62. C. Palmer, "SpaceX starship lands on earth, but manned missions to mars will require more," *Engineering* **7**, 1345–1347 (2021).
63. J. L. Heldmann, M. M. Marinova, D. S. Lim, *et al.*, "Mission architecture using the SpaceX starship vehicle to enable a sustained human presence on mars," *New Space* **10**, 259–273 (2022).
64. P. Jožič, A. Zidanšek, and R. Repnik, "Fuel conservation for launch vehicles: Falcon heavy case study," *Energies* **13**, 660 (2020).
65. G. Lao Rosell, "Study of commercial reusable launch vehicles business model: case study of New Glenn from Blue Origin," B.S. thesis (Universitat Politècnica de Catalunya, 2024).
66. C. Lee, "Heavy lift rocket competition coming to conclusion," *Natl. Def.* **105**, 29 (2020).
67. T. R. Brashears, "Achieving 99% link uptime on a fleet of 100g space laser inter-satellite links in Leo," *Proc SPIE* **12877**, 1287702 (2024).
68. A. U. Chaudhry and H. Yanikomeroglu, "Laser intersatellite links in a Starlink constellation: a classification and analysis," *IEEE Veh. Technol. Mag.* **16**, 48–56 (2021).
69. Y. Henri, "The OneWeb satellite system," in *Handbook of Small Satellites: Technology, Design, Manufacture, Applications, Economics and Regulation* (Springer, 2020), pp. 1091–1100.
70. O. B. Osoro and E. J. Oughton, "A techno-economic framework for satellite networks applied to low earth orbit constellations: assessing Starlink, OneWeb and Kuiper," *IEEE Access* **9**, 141611–141625 (2021).
71. S. Goswami, "Photonic quantum technologies: non-destructive photon detection and quantum simulation in solid-state systems," Ph.D. thesis (University of Calgary, 2021).
72. Y. Lei, F. Kimiaee Asadi, T. Zhong, *et al.*, "Quantum optical memory for entanglement distribution," *Optica* **10**, 1511 (2023).
73. X.-J. Wang, S.-J. Yang, P.-F. Sun, *et al.*, "Cavity-enhanced atom-photon entanglement with subsecond lifetime," *Phys. Rev. Lett.* **126**, 090501 (2021).
74. M. Körber, O. Morin, S. Langenfeld, *et al.*, "Decoherence-protected memory for a single-photon qubit," *Nat. Photon.* **12**, 18–21 (2018).
75. Y. Ma, Y.-Z. Ma, Z.-Q. Zhou, *et al.*, "One-hour coherent optical storage in an atomic frequency comb memory," *Nat. Commun.* **12**, 2381 (2021).
76. Y.-F. Hsiao, P.-J. Tsai, H.-S. Chen, *et al.*, "Highly efficient coherent optical memory based on electromagnetically induced transparency," *Phys. Rev. Lett.* **120**, 183602 (2018).
77. Y. Wang, J. Li, S. Zhang, *et al.*, "Efficient quantum memory for single-photon polarization qubits," *Nat. Photon.* **13**, 346–351 (2019).
78. S.-H. Wei, B. Jing, X.-Y. Zhang, *et al.*, "Quantum storage of 1650 modes of single photons at telecom wavelength," *NPJ Quantum Inf.* **10**, 19 (2024).
79. M. Bonarota, J.-L. Le Gouët, and T. Chanelière, "Highly multimode storage in a crystal," *New J. Phys.* **13**, 013013 (2011).
80. N. Sinclair, E. Saglamyurek, H. Mallahzadeh, *et al.*, "Spectral multiplexing for scalable quantum photonics using an atomic frequency comb quantum memory and feed-forward control," *Phys. Rev. Lett.* **113**, 053603 (2014).
81. A. Radnaev, Y. Dudin, R. Zhao, *et al.*, "A quantum memory with telecom-wavelength conversion," *Nat. Phys.* **6**, 894–899 (2010).
82. S. Wein, K. Heshami, C. A. Fuchs, *et al.*, "Efficiency of an enhanced linear optical Bell-state measurement scheme with realistic imperfections," *Phys. Rev. A* **94**, 032332 (2016).
83. L. Jiang, J. M. Taylor, and M. D. Lukin, "Fast and robust approach to long-distance quantum communication with atomic ensembles," *Phys. Rev. A* **76**, 012301 (2007).
84. Z.-B. Chen, B. Zhao, Y.-A. Chen, *et al.*, "Fault-tolerant quantum repeater with atomic ensembles and linear optics," *Phys. Rev. A* **76**, 022329 (2007).
85. C. Simon, H. de Riedmatten, M. Afzelius, *et al.*, "Quantum repeaters with photon pair sources and multimode memories," *Phys. Rev. Lett.* **98**, 190503 (2007).
86. O. A. Collins, S. D. Jenkins, A. Kuzmich, *et al.*, "Multiplexed memory-insensitive quantum repeaters," *Phys. Rev. Lett.* **98**, 060502 (2007).
87. K. Azuma, S. E. Economou, D. Elkouss, *et al.*, "Quantum repeaters: from quantum networks to the quantum internet," *Rev. Mod. Phys.* **95**, 045006 (2023).
88. J. Fekete, D. Rieländer, M. Cristiani, *et al.*, "Ultrannarrow-band photon-pair source compatible with solid state quantum memories and telecommunication networks," *Phys. Rev. Lett.* **110**, 220502 (2013).
89. M. Afzelius, C. Simon, H. De Riedmatten, *et al.*, "Multimode quantum memory based on atomic frequency combs," *Phys. Rev. A* **79**, 052329 (2009).
90. M. Afzelius, M. U. Staudt, H. De Riedmatten, *et al.*, "Efficient optical pumping of Zeeman spin levels in nd³⁺: Yvo₄," *J. Lumin.* **130**, 1566 (2010).
91. S. D. Barrett and P. Kok, "Efficient high-fidelity quantum computation using matter qubits and linear optics," *Phys. Rev. A* **71**, 060310 (2005).
92. M. Pompili, S. L. N. Hermans, S. Baier, *et al.*, "Realization of a multimode quantum network of remote solid-state qubits," *Science* **372**, 259–264 (2021).
93. A. Deltel, Z. Sun, W.-b. Gao, *et al.*, "Generation of heralded entanglement between distant hole spins," *Nat. Phys.* **12**, 218 (2016).
94. R. Stockill, M. J. Stanley, L. Huthmacher, *et al.*, "Phase-tuned entangled state generation between distant spin qubits," *Phys. Rev. Lett.* **119**, 010503 (2017).
95. V. Krutyanskiy, M. Galli, V. Krcmarsky, *et al.*, "Entanglement of trapped-ion qubits separated by 230 meters," *Phys. Rev. Lett.* **130**, 050803 (2023).
96. W. Rosenfeld, D. Burchardt, R. Garthoff, *et al.*, "Event-ready Bell test using entangled atoms simultaneously closing detection and locality loopholes," *Phys. Rev. Lett.* **119**, 010402 (2017).
97. J. Borregaard, P. Kómár, E. M. Kessler, *et al.*, "Long-distance entanglement distribution using individual atoms in optical cavities," *Phys. Rev. A* **92**, 012307 (2015).
98. S. Langenfeld, P. Thomas, O. Morin, *et al.*, "Quantum repeater node demonstrating unconditionally secure key distribution," *Phys. Rev. Lett.* **126**, 230506 (2021).
99. Y. Yu, F. Ma, X.-Y. Luo, *et al.*, "Entanglement of two quantum memories via fibres over dozens of kilometres," *Nature* **578**, 240–245 (2020).
100. J.-L. Liu, X.-Y. Luo, Y. Yu, *et al.*, "Creation of memory-memory entanglement in a metropolitan quantum network," *Nature* **629**, 579–585 (2024).
101. A. J. Stolk, K. L. van der Eenden, M.-C. Slater, *et al.*, "Metropolitan-scale heralded entanglement of solid-state qubits," *Sci. Adv.* **10**, eadp6442 (2024).
102. D. Castelvecchi, "Quantum internet' demonstration in cities is most advanced yet," *Nature* **629**, 734–735 (2024).
103. S. Pirandola, "Satellite quantum communications: fundamental bounds and practical security," *Phys. Rev. Res.* **3**, 023130 (2021).
104. R. M. Gagliardi, *Satellite Communications* (Springer Science & Business Media, 2012).

105. J.-P. Bourgoin, E. Meyer-Scott, B. L. Higgins, *et al.*, "A comprehensive design and performance analysis of low earth orbit satellite quantum communication," *New J. Phys.* **15**, 023006 (2013).
106. F. Kasten and A. T. Young, "Revised optical air mass tables and approximation formula," *Appl. Opt.* **28**, 4735–4738 (1989).
107. C. J. Pugh, J.-F. Lavigne, J.-P. Bourgoin, *et al.*, "Adaptive optics benefit for quantum key distribution uplink from ground to a satellite," *Adv. Opt. Technol.* **9**, 263–273 (2020).
108. E. Villaseñor, M. He, Z. Wang, *et al.*, "Enhanced uplink quantum communication with satellites via downlink channels," *IEEE Trans. Quantum Eng.* **2**, 1 (2021).
109. M. G. Raymer and K. Banaszek, "Time-frequency optical filtering: efficiency vs. temporal-mode discrimination in incoherent and coherent implementations," *Optics Express* **28**, 32819–32836 (2020).
110. S.-K. Liao, H.-L. Yong, C. Liu, *et al.*, "Long-distance free-space quantum key distribution in daylight towards inter-satellite communication," *Nat. Photon.* **11**, 509 (2017).
111. M. Abasifard, C. Cholsuk, R. G. Pousa, *et al.*, "The ideal wavelength for daylight free-space quantum key distribution," *APL Quantum* **1**, 016113 (2024).
112. M. T. Gruneisen, M. L. Eickhoff, S. C. Newey, *et al.*, "Adaptive-optics-enabled quantum communication: a technique for daytime space-to-earth links," *Phys. Rev. Appl.* **16**, 014067 (2021).
113. C. Bonato, A. Tomaello, V. D. Deppo, *et al.*, "Feasibility of satellite quantum key distribution," *New J. Phys.* **11**, 045017 (2009).
114. G. Vallone, D. Bacco, D. Dequal, *et al.*, "Experimental satellite quantum communications," *Phys. Rev. Lett.* **115**, 040502 (2015).
115. G. Vallone, D. Dequal, M. Tomasin, *et al.*, "Interference at the single photon level along satellite-ground channels," *Phys. Rev. Lett.* **116**, 253601 (2016).
116. C. Agnesi, F. Vedovato, M. Schiavon, *et al.*, "Philosophical transactions of the Royal Society A: mathematical," *Phys. Eng. Sci.* **376**, 20170461 (2018).
117. F. Vedovato, C. Agnesi, M. Schiavon, *et al.*, "Extending wheeler's delayed-choice experiment to space," *Sci. Adv.* **3**, e1701180 (2017).
118. M. Toyoshima, H. Takenaka, Y. Shoji, *et al.*, "Polarization measurements through space-to-ground atmospheric propagation paths by using a highly polarized laser source in space," *Opt. Express* **17**, 22333–22340 (2009).
119. R. Bedington, J. M. Arrazola, and A. Ling, "Progress in satellite quantum key distribution," *NPJ Quantum Inf.* **3**, 30 (2017).
120. J. Yin, Y. Cao, Y.-H. Li, *et al.*, "Satellite-to-ground entanglement-based quantum key distribution," *Phys. Rev. Lett.* **119**, 200501 (2017).
121. C.-Y. Lu, Y. Cao, C.-Z. Peng, *et al.*, "Micius quantum experiments in space," *Rev. Mod. Phys.* **94**, 035001 (2022).
122. Y.-A. Chen, Q. Zhang, T.-Y. Chen, *et al.*, "An integrated space-to-ground quantum communication network over 4,600 kilometres," *Nature* **589**, 214–219 (2021).
123. A. Jones, "China to launch new quantum communications satellites in 2025," *Space News* (2024). <https://spacenews.com/china-to-launch-new-quantum-communications-satellites-in-2025/>.
124. Y. Li, W.-Q. Cai, J.-G. Ren, *et al.*, "Microsatellite-based real-time quantum key distribution," *arXiv* (2024).
125. A. Villar, A. Lohrmann, X. Bai, *et al.*, "Entanglement demonstration on board a nano-satellite," *Optica* **7**, 734 (2020).
126. T. Jennewein, C. Simon, A. Fougères, *et al.*, "Qeysat 2.0—white paper on satellite-based quantum communication missions in Canada," *arXiv* (2023).
127. T. D. Jennewein, "Qeysat: Canada's first quantum communication satellite," *Proc. SPIE* **PC13106**, PC1310604 (2024).
128. A. M. Lewis and M. Travagnin, "A secure quantum communications infrastructure for Europe: technical background for a policy vision," (Publications Office of the European Union: Luxembourg, 2022).
129. R. Kaltenbaek, A. Acin, L. Bacsardi, *et al.*, "Quantum technologies in space," *Exp. Astron.* **51**, 1677–1694 (2021).
130. G. C. Rivera, O. Heirich, A. Shrestha, *et al.*, "Building Europe's first space-based quantum key distribution system—the German aerospace center's role in the EAGLE-1 mission," *arXiv* (2024).
131. K. Ortiz, L. Ramsey, S. Johnson, *et al.*, "Seaque: a polarization-entanglement quantum payload," (Bulletin of the American Physical Society, 2024).
132. R. P. Singh, "How India plans to make satellite communication hack-proof," *Nature India* (2023).
133. L. Calderaro, C. Agnesi, D. Dequal, *et al.*, "Towards quantum communication from global navigation satellite system," *Quantum Sci. Technol.* **4**, 015012 (2018).
134. V. B. Braginsky, Y. I. Vorontsov, and K. S. Thorne, "Quantum nondemolition measurements," *Science* **209**, 547–557 (1980).
135. P. Grangier, J. A. Levenson, and J.-P. Poizat, "Quantum nondemolition measurements in optics," *Nature* **396**, 537–542 (1998).
136. S. Goswami, K. Heshami, and C. Simon, "Theory of cavity-enhanced nondestructive detection of photonic qubits in a solid-state atomic ensemble," *Phys. Rev. A* **98**, 043842 (2018).
137. C. O'Brien, T. Zhong, A. Faraon, *et al.*, "Nondestructive photon detection using a single rare-earth ion coupled to a photonic cavity," *Phys. Rev. A* **94**, 043807 (2016).
138. A. Reiserer, S. Ritter, and G. Rempe, "Nondestructive detection of an optical photon," *Science* **342**, 1349–1351 (2013).
139. L. Liu, D.-S. Lü, W.-B. Chen, *et al.*, "In-orbit operation of an atomic clock based on laser-cooled 87Rb atoms," *Nat. Commun.* **9**, 2760 (2018).
140. D. C. Aveline, J. R. Williams, E. R. Elliott, *et al.*, "Observation of Bose-Einstein condensates in an Earth-orbiting research lab," *Nature* **582**, 193–197 (2020).
141. M. Gündoğan, T. Jennewein, F. K. Asadi, *et al.*, "Topical white paper: a case for quantum memories in space," *arXiv* (2021).
142. M. Jutisz, A. Erl, J. Wolters, *et al.*, "Stand-alone mobile quantum memory system," *Phys. Rev. Appl.* **23**, 024045 (2025).
143. J. Wallnöfer, F. Hahn, M. Gündoğan, *et al.*, "Simulating quantum repeater strategies for multiple satellites," *Commun. Phys.* **5**, 169 (2022).
144. V. D. Tubío, M. B. Aldecocea, J. van Dam, *et al.*, "Satellite-assisted quantum communication with single photon sources and atomic memories," *arXiv* (2024).
145. K. Azuma, H. Takeda, M. Koashi, *et al.*, "Quantum repeaters and computation by a single module: remote nondestructive parity measurement," *Phys. Rev. A At. Mol. Opt. Phys.* **85**, 062309 (2012).
146. S. E. Wittig, S. M. Wittig, A. Berquanda, *et al.*, "Concept for single-satellite global quantum key distribution using a solid state quantum memory," IAC-17,B2,7,1,x36863. <http://iafaastro.directory/iac/paper/id/36863/summary/> (2017).
147. M. Zhong, M. P. Hedges, R. L. Ahlefeldt, *et al.*, "Optically addressable nuclear spins in a solid with a six-hour coherence time," *Nature* **517**, 177–180 (2015).
148. F. Wang, M. Ren, W. Sun, *et al.*, "Nuclear spins in a solid exceeding 10-hour coherence times for ultra-long-term quantum storage," *PRX Quantum* **6**, 010302 (2025).
149. A. Seri, D. Lago-Rivera, A. Lenhard, *et al.*, "Quantum storage of frequency-multiplexed heralded single photons," *Phys. Rev. Lett.* **123**, 080502 (2019).
150. E. Da Ros, S. Kanthak, E. Sağlamyürek, *et al.*, "Proposal for a long-lived quantum memory using matter-wave optics with bose-einstein condensates in microgravity," *Phys. Rev. Res.* **5**, 033003 (2023).
151. Y. Li and E. Wolf, "Focal shifts in diffracted converging spherical waves," *Optics Commun.* **39**, 211–215 (1981).
152. K. F. Renk, *Basics of Laser Physics: For Students of Science and Engineering*, (Springer Science & Business Media, 2012).
153. L. Pinard, C. Michel, B. Sassolas, *et al.*, "Mirrors used in the LIGO interferometers for first detection of gravitational waves," *Appl. Opt.* **56**, C11–C15 (2017).
154. H.-Y. Liu, X.-H. Tian, C. Gu, *et al.*, "Optical-relayed entanglement distribution using drones as mobile nodes," *Phys. Rev. Lett.* **126**, 020503 (2021).
155. M. Aspelmeyer, T. Jennewein, M. Pfennigbauer, *et al.*, "Long-distance quantum communication with entangled photons using satellites," *IEEE J. Sel. Top. Quantum Electron.* **9**, 1541–1551 (2003).
156. D. Dequal, G. Vallone, D. Bacco, *et al.*, "Experimental single-photon exchange along a space link of 7000 km," *Phys. Rev. A* **93**, 010301 (2016).

157. M. Guelman, A. Kogan, A. Kazarian, *et al.*, "Acquisition and pointing control for inter-satellite laser communications," *IEEE Trans. Aerosp. Electron. Syst.* **40**, 1239–1248 (2004).
158. K. S. Lakshmi, M. S. Kumar, and K. Kavitha, "Inter-satellite laser communication system," in *2008 International Conference on Computer and Communication Engineering* (IEEE, 2008), pp. 978–983.
159. A. U. Chaudhry and H. Yanikomeroglu, "Temporary laser inter-satellite links in free-space optical satellite networks," *IEEE Open J. Commun. Soc.* **3**, 1413–1427 (2022).
160. A. N. Kolmogorov, "The local structure of turbulence in incompressible viscous fluid for very large Reynolds Numbers," In *Dokl. Akad. Nauk SSSR* **30**, 301 (1941).
161. H. Gu, R. Yu, Z. Li, *et al.*, "Quesat: satellite-assisted quantum internet for global-scale entanglement distribution," *arXiv* (2025).
162. W. T. Welford and R. Winston, *Optics of Nonimaging Concentrators. Light and Solar Energy* (Academic Press Incorporated, 1978).
163. T. Markvart, "The thermodynamics of optical étendue," *J. Opt. A: pure Appl. Opt.* **10**, 015008 (2008).
164. B. Abbott, R. Abbott, R. Adhikari, *et al.*, "LIGO: the laser interferometer gravitational-wave observatory," *Rep. Prog. Phys.* **72**, 076901 (2009).